Surface modification of aluminum doped zinc oxide (AZO) anodes with CF_x plasma treatment and nanoscale WO_x layers for enhanced electro-optical performance in OLEDs

Jitendra Kumar Jha, Reinaldo Santos-Ortiz, Wei Sun, Jincheng Du and Nigel D. Shepherd*

Department of Materials Science and Engineering, University of North Texas, Denton, Texas 76201.
*Email: Nigel.shepherd@unt.edu

Abstract

Aluminum doped zinc oxide (AZO) films were subjected to carbon tetra-fluoride (CF_4) plasma treatment and deposition of tungsten sub-oxide (WO_x) surface layers to evaluate the impact on its workfunction, for application as transparent conducting oxide (TCO) anodes in organic light emitting diodes (OLEDs). Ultraviolet photoelectron spectroscopy (UPS) revealed that CF_x plasma treatment improved the workfunction of AZO from 4.1 eV to 4.5 eV and that deposition of nanoscopic (~ 3 nm) WO_x surface layers resulted in an effective workfunction of 4.7 eV for the AZO/WO_x stack. The increase in workfunction with plasma treatment is due to increased electronegativity of the surface, and reinforcement of the existing surface dipole. Gap states in the higher workfunction WO_x layer determine the effective workfunction of the AZO/WO_x (3nm) composite. The performance of surface modified AZO anodes was compared to standard indium tin oxide (ITO) in simple bilayer OLEDs with tris(8-hydroquinoline) aluminum (AlQ_3) as the emissive and electron-transport layer, and N,N'-Bis (naphthalene-1-yl)–N,N'-bis(phenyl)-benzidine (NPB) as the hole transport layer. At 9 V applied, OLEDs with AZO/WO_x (3 nm) anodes exhibited luminous efficiency (LE), power efficiency (PE), and external quantum efficiency (EQE) of 4.7 Cd/A, 1.6 lm/W and 1.5 % respectively, which were higher than the 2.4 Cd/A, 0.9 lm/W and 0.9 % from OLEDs with standard ITO anodes. OLEDs with CF_x plasma treated AZO anodes demonstrated LE, PE, and EQE of 2.3 Cd/A, 0.8 lm/W and 0.8 %, respectively, which were higher than as-deposited AZO, but smaller than ITO. The improved efficiency of the AZO/WO_x devices is ascribed to better band alignment (between the anode and NPB), hole injection, and charge balance compared to standard ITO.

Keywords: Aluminum-zinc oxide, Surface modification, Workfunction tuning, Hole injection, High efficiency, OLED.

1. Introduction

More extensive commercialization of organic light emitting diode (OLED) technology in solid state lighting and display technology [1] require efficiency and lifetime improvements, as well as cost reductions, inclusive of the transparent conducting oxide (TCO). Indium tin oxide is the standard transparent conducting oxide (TCO) anode in OLEDs [2,3]. However, indium is expensive and the Earth's reserve of this element is limited. Thus, the extensive research to find alternative TCOs is well warranted. Zinc oxide (ZnO) and its variants such as aluminum doped ZnO (AZO) exhibit comparable electrical conductivity and transmissivity to ITO, and are of interest for TCO applications. However, the workfunction of ZnO and AZO is smaller compared to ITO [4] . The smaller workfunction of AZO results in a higher hole injection barrier at the anode/organic interface, and thus a higher turn-on voltage and degraded electro-optical performance of AZO based OLEDs compared to ITO can be expected. In previous reports, we demonstrated workfunction improvements by surface modification using O_2 plasma, or, molybdenum oxide (MoO_x) interfacial layers, and discussed the mechanisms which resulted in enhanced hole injection efficiency [5,6]. In the present work, we report the performance of CF_x plasma treated AZO and AZO/WO_x anodes in OLEDs, and demonstrate that with workfunction tuning their performance is comparable to the ITO standard.

2. Experiment

Radio Frequency (rf) sputtering of a 99.99% pure, ZnO doped with 2% Al_2O_3 target, was used for depositing AZO thin-films onto cleaned AF-45 display glass substrates. The deposition conditions for optimal AZO electrical conductivity and transmissivity have been reported [4]. CF_x plasma treatment was carried out in a MPS200 RIE chamber at a rf frequency of 13.56 MHz. The base pressure was 10^{-6} Torr, and plasma treatment was performed for 20 seconds using 50 mTorr of CF_4 and 60 W of power. WO_x films were deposited onto O_2 plasma treated AZO films by thermal evaporation of tungsten oxide (WO_3) powder using the technique previously reported [5].

OLEDs were processed on CF_x plasma treated AZO, AZO with 3 nm WO_x surface layers, and O_2 plasma treated ITO substrates. Thus, Device 1 had an AZO (CF_x plasma treated) anode, in Device 2 the anode was AZO/WO_x and in Device 3 the anode was the ITO control. In all devices the NPB hole transport layer was 60nm, the AlQ_3 layer was 40nm, and the cathodes were LiF (1 nm)/Al (100 nm). We have previously reported the OLED fabrication procedures [7], UPS measurement methodology [5], and device measurement [8].

Table 1: Summary of calculated workfunction from UPS measurement of as-deposited AZO, CF_x plasma treated AZO, O_2 plasma treated AZO/WO_x (3 nm), and O_2 plasma treated ITO. Electro-optical performance parameters of the OLED devices fabricated with different anode configurations.

Devices	Anode workfunction (eV)	OLED [Anode/NPB(60nm)/AlQ_3(40nm)/LiF:Al]	$V_{turn-on}$ (V) (@ 1 Cd/m^2)	@ 9V		
1. AZO (as-deposited)	4.1			Brightness (Cd/m^2)	PE (lm/W)	EQE (%)
3.AZO(CF_x plasma treated)	4.5	Device 1	2.6	4748	1.16	1.09
4.AZO(O_2 plasma treated)/WO_x(3nm)	4.7	Device 2	2.5	7009	1.6	1.6
5.ITO (O_2 plasma treated)	4.6	Device 3	2.6	9685	0.84	0.83

3. Result and Discussion

Figure 1(a) shows the UPS spectra of the surface modified AZO films. The measured workfunction are presented in Table 1, along with that of the ITO control and as-deposited AZO. The secondary electron cut-off of the CF_x plasma treated and AZO films with a WO_x interfacial layer are shifted towards lower binding energy compared to the as-deposited AZO films, indicating increased workfunction.

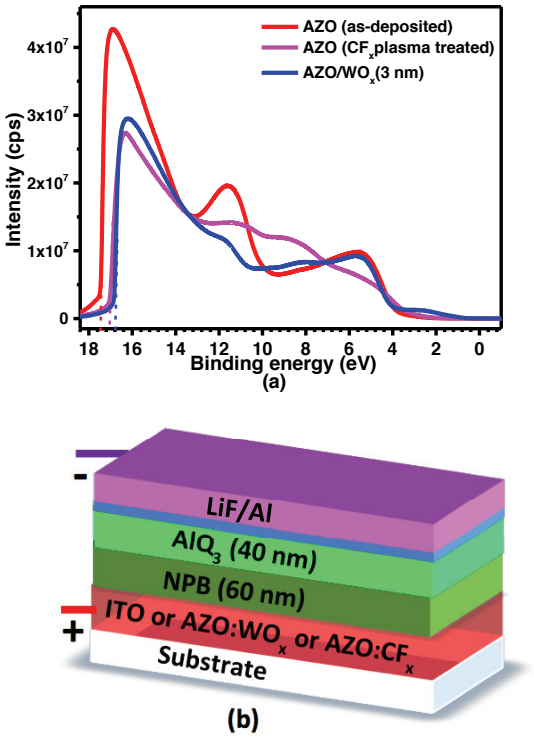

Figure 1: (a) UPS spectra of as-deposited AZO, CF_x plasma treated AZO and AZO/WO_x (3 nm) films. (b) Schematic structure of the bilayer OLED.

We previously showed using density functional theory (DFT) that the workfunction of ZnO films increased upon adsorption of F or CF_3 groups, due to the created electronegative environment [9]. The mechanism of CF_x plasma treatment of AZO surfaces is similar, with electronegative fluorine causing a surface charge redistribution, and, an associated dipole moment that reinforces the original surface dipole moment of the AZO, resulting in increased workfunction. The workfunction of as-deposited AZO film increased from 4.1 eV to 4.7 eV upon deposition of a 3 nm WO_x surface layer, which is due to the workfunction of WO_x layer itself [5, 10]. These increases in workfunction are expected to translate into a reduction of the hole injection barrier compared to as-deposited AZO.

A schematic of the OLEDs fabricated to evaluate the anode performance is shown in Figure 1(b). OLEDs were not fabricated with the low workfunction, 4.1 eV, as-deposited AZO. Current density (J) and luminance (L) vs voltage (V) plots for the OLEDs are shown in Figure 2. Device 3 had the highest luminance and current density. Voltage drops and charge trapping at the AZO/NPB or AZO/WO_x/NPB interfaces as well as higher resistivity of the AZO anode (compared to ITO) are likely contributors to this effect [11-13]. The electroluminescence spectrum of the OLEDs is characteristic of AlQ_3, and is shown in the inset of Figure 4 [14]. The higher luminance of the device with the standard ITO anode follows the higher current density.

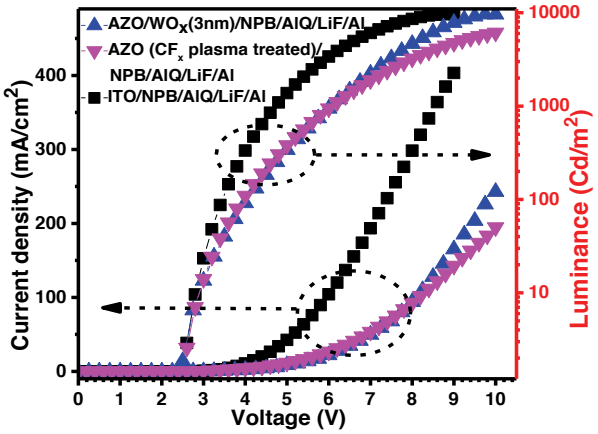

Figure 2: Current density vs Voltage (V) plot of Devices 1, 2, 3, and, Luminance (L) vs voltage (V) plots of Devices 1, 2, and 3.

The PE and EQE vs J data of the devices are shown in Figure 3(a) and 3(b). The PE and EQE of the devices were calculated from the L vs V and J vs V data using the standard methodology [15], and are tabulated in Table 1. At 9 V, Device 2 exhibited a maximum PE of 1.6 lm/W, which is larger than 0.84 lm/W obtained from standard ITO (Device 3). Device 2 also displayed the highest EQE (%) among all the devices. The EQE (%) of Device 1 was observed to be almost equivalent to Device 3, the ITO control. We ascribe the improved performance of the AZO/WO_x (3 nm) anode to improved charge balance and enhanced radiative recombination kinetics, compared to ITO.

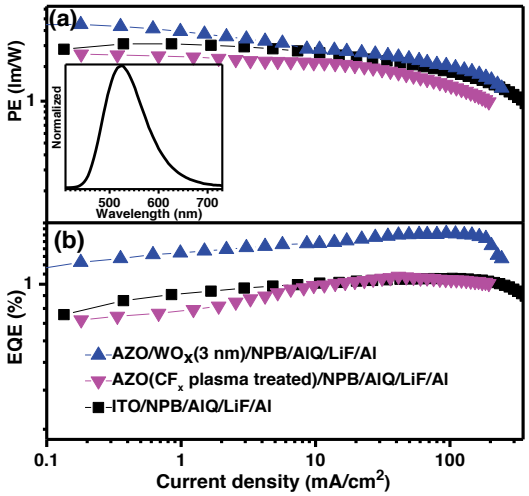

Figure 3: (a) Power efficiency (PE) vs Current density (J), and (b) External quantum efficiency (EQE) vs Current density (J) plots of Devices 1, 2, and 3. Inset shows electroluminescence spectrum of all the OLED devices.

4. Conclusion

Deposition of nanoscopic, higher workfunction WO_x layers onto AZO increased the effective workfunction of AZO/WO_x (3nm) composite anodes. CF_x plasma treatment of AZO films increased its workfunction due to a fluorinated, electronegative surface that results in a dipole moment that enhances the original surface dipole. Electro-optical characterization of OLEDs fabricated using surface modified AZO anodes revealed that the PE and EQE of AZO/WO_x (3 nm) based OLEDs was better than standard ITO. The larger workfunction of AZO/WO_x (3 nm) anode enhanced hole injection and charge balance in the recombination zone, leading to better efficiencies.

Acknowledgements

This work is sponsored by National Science Foundation under grant No. 1234978.

References

[1] B. Geffroy, P. Le Roy, C. Prat, Organic light-emitting diode (OLED) technology: materials, devices and display technologies, Polym. Int. 55 (2006) 572-582.

[2] M. Lin, M. Li, W. Chen, M.A. Omary, N.D. Shepherd, Transient electroluminescence determination of carrier mobility and charge trapping effects in heavily doped phosphorescent organic light-emitting diodes, Solid-State Electron. 56 (2011) 196-200.

[3] M. Li, W. Chen, M. Lin, M.A. Omary, N.D. Shepherd, Near-white and tunable electrophosphorescence from bis[3,5-bis(2-pyridyl)-1,2,4-triazolato]platinum(II)-based organic light emitting diodes, Org. Electron. 10 (2009) 863-870.

[4] Jitendra Kumar Jha, Reinaldo Santos-Ortiz, Jincheng Du, and Nigel D. Shepherd, Semiconductor to metal transition in degenerate ZnO: Al films and the impact on its carrier scattering mechanisms and bandgap for OLED applications, J. Mater. Sci: Mater. Electron. 25 (2014) 1492.

[5] J.K. Jha, R. Santos-Ortiz, J. Du, N.D. Shepherd, The influence of MoOx gap states on hole injection from aluminum doped zinc oxide with nanoscale MoOx surface layer anodes for organic light emitting diodes, J. Appl. Phys. 118 (2015) 065304.

[6] Fang-Ling Kuo, Yun Li, Marvin Solomon, Jincheng Du, and Nigel, D. Shepherd, Workfunction tuning of zinc oxide films by argon sputtering and oxygen plasma: an experimental and computational study, J. Phys. D: Appl. Phys. 45 (2012) 065301.

[7] M. Li, W. Chen, M. Lin, I. Oswald, M. Omary, N.D. Shepherd, High efficiency electrophosphorescence from bilayer organic light emitting diodes, J. Phys. D: Appl. Phys. 44 (2011) 365103.

[8] M. Li, M. Lin, W. Chen, R. McDougald, R. Arvapally, M. Omary, N.D. Shepherd, High efficiency orange-red phosphorescent organic light emitting diodes based on a Pt(II)-pyridyltriazolate complex from a structure optimized for charge balance and reduced efficiency roll-off, physica status solidi (a). 209 (2012) 221-225.

[9] W. Sun, Y. Li, J.K. Jha, N.D. Shepherd, J. Du, Effect of surface adsorption and non-stoichiometry on the workfunction of ZnO surfaces: A first principles study, J. Appl. Phys. 117 (2015) 165304.

[10] C. Tao, S. Ruan, G. Xie, X. Kong, L. Shen, F. Meng, C. Liu, X. Zhang, W. Dong, W. Chen, Role of tungsten oxide in inverted polymer solar cells, Appl. Phys. Lett. 94 (2009) 043311-1-043311-3.

[11] H. Lu, C. Tsou, M. Yokoyama, Organic light-emitting devices with energy-level aligned double-buffer layers, J. Cryst. Growth. 289 (2006) 161-163.

[12] S.M. Sze, K.K. Ng, Physics of Semiconductor Devices, Third edition ed., John Wiley & Sons, 2007.

[13] A. Benor, S. Takizawa, C. Pérez-Bolivar, P. Anzenbacher Jr, Energy barrier, charge carrier balance, and performance improvement in organic light-emitting diodes, Appl. Phys. Lett. 96 (2010) 243310.

[14] D. Poitras, C. Kuo, C. Py, Design of high-contrast OLEDs with microcavity effect, Optics express. 16 (2008) 8003-8015.

[15] S.R. Forrest, D.D. Bradley, M.E. Thompson, Measuring the Efficiency of Organic Light-Emitting Devices, Adv Mater. 15 (2003) 1043-1048.